Non-Uniformity of Wafer and Pad in CMP: Kinematic Aspects of View

Feng Tyan

Computational Dynamics and Control Lab

Dept. of Aerospace Engineering

Tamkang University

Tamshui, Taipei County, Taiwan 25147, R. O. C.

Abstract— In this paper, we analyze the non-uniformity of sliding distance on both wafer and polishing pad from kinematic point of view. Use the Fourier series expansion, we can show that in steady state the non-uniformity is determined by the ratio between rotary speeds of platen and wafer carrier (m), and the ratio of wafer radius to the distance between the center of platen and wafer ($\frac{R_c}{d}$). In general, the non-uniformity of wafer increases with $|m|$ and $\frac{R_c}{d}$. An important observation for polishing pad is that in two particular ranges of the ratio m, the larger $\frac{R_c}{d}$ produces the smaller non-uniformity. Then a ring type polishing pad is proposed for the purpose of improving the non-uniformity of both wafer and pad. However, it turns out that the result is much worse than we expected.

I. INTRODUCTION

Chemical mechanical polishing/planarization (CMP) has emerged recently as a vital processing technique for a higher degree of planarization in submicron VLSI beyond the resolution of 0.35μm [1]. Although CMP has been widely used for a few years, the mechanism of the material removal is yet to be explored. The primary factors affecting planarization efficiency are mechanical (downforce on the wafer, platen speed, pad structure) and chemical (slurry chemistry). To improve throughput, material removal rate (MRR) is maximized. Removal rate and removal rate uniformity across a wafer are also strong functions of downforce, platen speed, pad structure and slurry chemistry. Among them, relative velocity distribution on the wafer surface is considered as an important factor affecting the spatial distribution of removal rate since it determines the sliding distance of given point on the wafer The early work of Runnels et al. [2] and Hocheng et al. [1, 3] had analyzed some aspects of kinematics in CMP. However, many topics still remain open in this area.

In this study we adopt two dimensionless parameters to analyze the non-uniformity of both wafer and pad. Namely, the ratio between rotational speeds of wafer carrier and platen (m) and the ratio of wafer radius to the distance between the center of platen and wafer. At first, a classic kinematic mehtod is implemented to derive the relative velocity at the contact point in the first part of section II. Then a dimensionless sliding distance and the related non-uniformity is defined and determined as the performance index for the polishing result.

Finally a ring type polishing pad is proposed for the purpose of improving the non-uniformity of both wafer and pad. However, it turns out that the result is much worse than we expected.

II. KINEMATIC ANALYSIS OF RELATIVE VELOCITY DISTRIBUTION

Fig. 1 depicts a typical CMP schematic, and Fig. 2 shows the definitions of the kinematic parameters of CMP, in which $\vec{L}_p$ is the position vector of point p relative to pad center, $\vec{L}_c$ is the position vector measured from carrier center, and $\vec{d} = d\vec{i}$ is the postilion vetoer of carrier center measured from carrier center, $\vec{i}$ is a unit vector along $\vec{d}$. In this figure, the pad and wafer are rotating with angular velocities $\vec{\omega}_p = \omega_p \vec{k}$ and $\vec{\omega}_c = \omega_c \vec{k}$ respectively, where $\vec{k}$ is the unit vector orthogonal to wafer and pad surface.
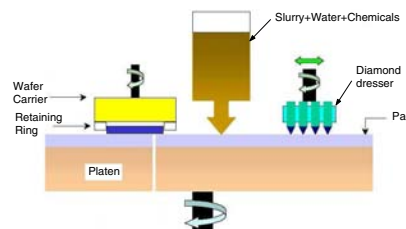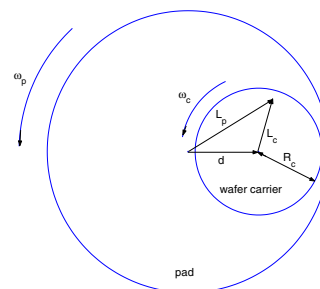

Fig. 1. CMP Schematic

Fig. 2. The kinematic parameters of the CMP (top view)

The well known Preston equation, empirically found from the experiment of the glass polishing in 1927, has been

proposed to predict the material removal rate of CMP [1, 4]. According to the Preston equation, the material removal rate

$$\dot{M} = -\kappa_p P V, \tag{2.1}$$

where P is the contact pressure distribution at contact point, V is the magnitude of the relative velocity at contact point p between wafer and polishing pad and κ_p is a constant representing the effect of the other remaining parameters including the chemical reaction, pad property, ..., and so on [5].

Now we are going to express the relative velocity in terms of the parameters of wafer. At any instant, the relative velocity $\vec{v}$ between pad and carrier at any contact point p is

$$\begin{aligned} \vec{v} &= \vec{v}_p - \vec{v}_c = \vec{\omega}_p \times (\vec{d} + \vec{L}_c) - \vec{\omega}_c \times \vec{L}_c, \\ &= (\vec{\omega}_p - \vec{\omega}_c) \times \vec{L}_c + \vec{\omega}_p \times \vec{d}. \end{aligned} \tag{2.2}$$

Define the magnitude of $\vec{v}$ as $V \triangleq \|\vec{v}\|$. It can be shown that

$$V = \sqrt{\vec{v} \cdot \vec{v}} = \omega_c d \left\| (m-1)\rho_c \vec{e}_c + m\vec{i} \right\|, \tag{2.3}$$

where the dimensionless distance

$$\rho_c \triangleq \frac{\|\vec{L}_c\|}{d}, \tag{2.4}$$

and $\vec{e}_c$ is the unit vector in the direction of $\vec{L}_c$, m is defined as the ratio of rotational speeds,

$$m = \frac{\omega_p}{\omega_c}. \tag{2.5}$$

Note that negative m stands for wafer and pad rotate in opposite direction, and

$$\vec{e}_c \cdot \vec{i} = \cos(\omega_c t + \theta), \tag{2.6}$$

where θ is the initial angular position of the contact point on the wafer measured from $\vec{d}$.

Similarly, we can derive the distribution of the relative velocity on the pad as follows,

$$\begin{aligned} \vec{v} &= \vec{v}_p - \vec{v}_c \\ &= (\vec{\omega}_p - \vec{\omega}_c) \times \vec{L}_p + \vec{\omega}_c \times \vec{d}. \end{aligned} \tag{2.7}$$

It follows that the magnitude of relative velocity can be shown as

$$V = \omega_c d \left\| (m-1)\rho_p \vec{e}_p + \vec{i} \right\|, \tag{2.8}$$

where the dimensionless distance

$$\rho_p \triangleq \frac{\|\vec{L}_p\|}{d}, \tag{2.9}$$

$\vec{e}_p$ is the unit vector in the direction of $\vec{L}_p$, and

$$\vec{e}_p \cdot \vec{i} = \cos(\omega_p t + \phi), \tag{2.10}$$

ϕ is the initial angular position of the contact point on the polishing pad measured from $\vec{d}$.

Fig. 3 shows the normalized relative velocity distribution $\frac{V}{\omega_c d}$ at a particular instant for $m = 1.5$ on wafer and pad respectively, in both figures i-axis stands for the $\vec{d}$ direction, and j-axis is the direction of $\vec{k} \times \vec{i}$. From these two figures, we can see that both the inclination of the surfaces is $m - 1 = 0.5$ in this case.
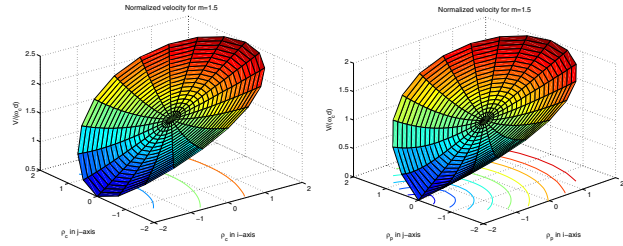

Fig. 3. The normalized relative velocity $\frac{V}{\omega_c d}$ on wafer and pad

A. *The Sliding Distance Distribution on the Wafer*

For convenience, we define the normalized sliding distance as

$$S_n(\rho_c, \theta, m) \triangleq \frac{1}{\omega_c d T} \int_0^T V \, dt, \tag{2.11}$$

where T is the elapsed time. Hence, if $\omega_p = \omega_c$, that is $m = 1$, then we have $V = \omega_c d$, and

$$S_n(\rho_c, \theta, 1) = 1, \tag{2.12}$$

which implies the magnitudes of the relative velocity is the same throughout the contact surface on the wafer [6, 7]. Henceforth, the wafer can achieve global planarization theoretically if the pressure distribution is uniform and no other effects are considered.

However, for $m \neq 1$, the normalized sliding distance can be obtained from the following

$$\begin{aligned} S_n(\rho_c, \theta, m) &= \frac{1}{\omega_c d T} \int_0^T V \, dt, \\ &= \frac{2|(m-1)\rho_c + m|}{\omega_c T} \int_{\frac{1}{2}\theta}^{\frac{1}{2}[\omega_c T + \theta]} \sqrt{1 - k_c \sin^2(\tau)} \, d\tau, \end{aligned} \tag{2.13}$$

where the parameter k_c is defined as

$$k_c \triangleq \frac{4(m-1)m\rho_c}{[(m-1)\rho_c + m]^2}. \tag{2.14}$$

Since the integrand of equation (2.13), $\sqrt{1 - k_c \sin^2(\tau)}$, is is an even periodic function with period π, we can write it as a Fourier series expansion

$$\sqrt{1 - k_c \sin^2(\tau)} = a_0 + \sum_{n=1}^{\infty} a_n \cos(2n\tau),$$

where $a_n, n = 0, 1, \ldots,$ are the corresponding Fourier coefficients. In particular, the coefficient

$$a_0 = \frac{2}{\pi} \int_0^{\frac{\pi}{2}} \sqrt{1 - k_c \sin^2(\tau)} \, d\tau. \tag{2.15}$$

It follows that as the elapsed time $T \to \infty$, i.e. in the steady state,

$$S_{ns}(\rho_c, m) \triangleq \lim_{T \to \infty} S_n(\rho_c, \theta, m)$$
$$= |(m-1)\rho_c + m|a_0. \tag{2.16}$$

The resulted normalized sliding distance here is identical to the one obtained by Chen and Lee [8], in which the result was obtained through a three link manipulator model. Fig. 4 clearly indicates that the larger the ρ_c is, the larger the normalized sliding distance will be. Hence, for fixed rotational ratio m, the material removal of wafer at the edge area is higher than that at the central area. This conclusion is consistent with the one given in [9] and the references therein. While in [9], the result was obtained through a Taylor series expansion, it is valid only for small ρ_c and $m \approx 1$.
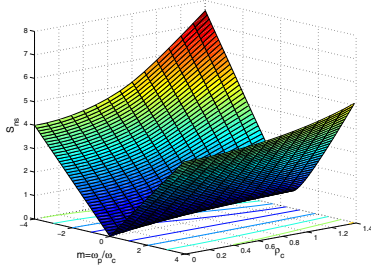

Fig. 4. The steady state normalized sliding distance $S_{ns}(\rho_c, m)$ on wafer.

B. The Sliding Distance Distribution on the Pad

Next, consider the material removed of pad at a specific point p. For a long enough period of elapsed time, T, the actual contact time, $T_c(\rho_p)$, between wafer and pad is (See Fig. 5)

$$T_c(\rho_p) = T \frac{2\theta_p(\rho_p)}{2\pi}, \tag{2.17}$$

where $\theta_p(\rho_p)$ can be found through vector analysis

$$\theta_p(\rho_p) = \begin{cases} \cos^{-1} \frac{1 + \rho_p^2 - \frac{R_c^2}{d^2}}{2\rho_p}, & 1 - \frac{R_c}{d} \le \rho_p \le 1 + \frac{R_c}{d} \\ 0, & \text{otherwise}, \end{cases}$$

in which ρ_p is defined by (2.9). Note that the maximum contact time occurs at $\rho_p = \sqrt{1 - \left(\frac{R_c}{d}\right)^2}$. Therefore, the normalized sliding distance of contact point p on the polishing pad for a period of elapsed time, T, can be calculated by

$$S_n(\rho_p, \phi, m) \triangleq \frac{1}{\omega_c dT} \int_0^{T_c(\rho_p)} V dt$$
$$= \frac{1}{T} \int_0^{T_c(\rho_c)} \left\| (m-1)\rho_p \vec{e}_p + \vec{i} \right\| dt$$
$$= \frac{2|(m-1)\rho_p + 1|}{\omega_p T}$$
$$\cdot \int_{\frac{1}{2}\phi}^{\frac{1}{2}(\omega_p T_c(\rho_p) + \phi)} \sqrt{1 - k_p \sin^2(\tau)} d\tau, \tag{2.18}$$

where

$$k_p = \frac{4(m-1)\rho_p}{[(m-1)\rho_p + 1]^2}. \tag{2.19}$$

Use the same reasons given in Section II-A, the steady state of the normalized sliding distance on the pad can be written as

$$S_{ns}(\rho_p, m) = |(m-1)\rho_p + 1| \frac{\theta_p(\rho_p)}{\pi} a_0, \tag{2.20}$$

where

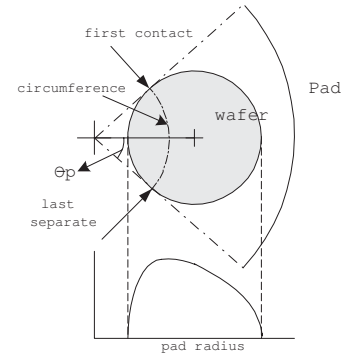$$a_0 = \frac{2}{\pi} \int_0^{\frac{\pi}{2}} \sqrt{1 - k_p \sin^2(\tau)} d\tau. \tag{2.21}$$

Fig. 5. Pad creep and recovery region and $\theta_p(\rho_p)$

According to the Preston's equation (2.1), pad wear is proportional to the sliding distance. Thus, the shape of deformation across the pad radius becomes uneven as polishing time goes on. This phenomenon can be observed from Fig. 6, in which we assume $\frac{R_c}{d} = \frac{2}{3}$.
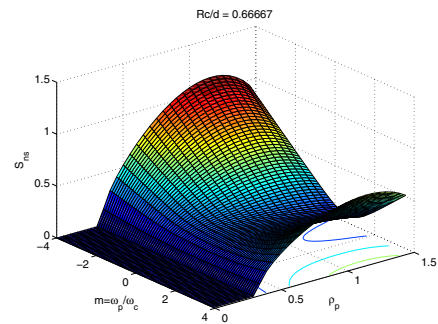

Fig. 6. The steady state normalized sliding distance $S_{ns}(\rho_p, m)$ on pad.

Although, the condition $\omega_p = \omega_c$ can be used to achieve the global planarization for wafer, if we only take into account the effect of relative velocity. However, the polishing pad still undergoes an uneven deformation, it will leave a *bowl shape* concavity on the pad surface [9]. This bowl shape concave will seriously affect the polishing process, because it directly change the contact surface profile, as a result will destroy the uniform contact pressure distribution that is required.

C. The Uniformity of Wafer and Pad

In this section, let us examine the effects of rotational speeds, $m = \frac{\omega_p}{\omega_c}$, and the distance between two centers, d. For comparison, let us define the *non-uniformity* (NU) as

$$\text{NU}(\frac{R_c}{d}, m) \triangleq \frac{\text{std}(S_{ns}(\rho, m))}{\text{mean}(S_{ns}(\rho, m))},$$

$$\begin{cases} 0 \le \rho \le \frac{R_c}{d}, & \text{for wafer,} \\ 1 - \frac{R_c}{d} \le \rho \le 1 + \frac{R_c}{d}, & \text{for pad} \end{cases}, \qquad (2.22)$$

to be our performance index, where "std" and "mean" are the standard deviation and mean of S_{ns} taken over the defined dimensionless radius ρ.
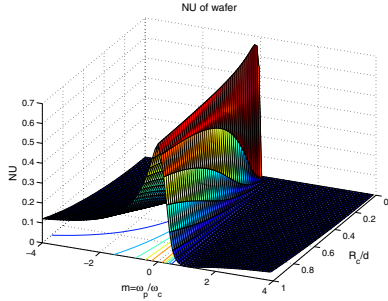

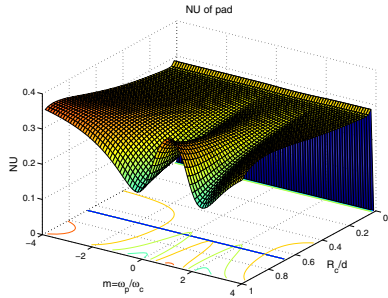Fig. 7. The non-uniformity of wafer vs. $\frac{R_c}{d}$ and m

Fig. 8. The non-uniformity of pad vs. $\frac{R_c}{d}$ and m

Figure 7 and 8 illustrate the numerical results for various values of ratio m and $\frac{R_c}{d}$. From these two figures, some conclusions can be drawn:

For the wafer surface:

1) When the ratio $m = 1$, we have $NU = 0$, which agrees with previous discussion, while for $m < 1$, the non-uniformity of wafer surface increases rapidly. Negative m gives much higher value of NU than positive m does.

2) The non-uniformity increases as $\frac{R_c}{d}$ increases, that is, either the size of the wafer is larger or the centers between the pad and wafer is closer.

For polishing pad surface:

1) For $m > 0$ the minimum value of NU of pad occurs at $m \approx 2$, while for $m < 0$, the minimum non-uniformity occurs at $m \approx -0.5$.

2) For two particular ranges of values of m, (e.g. $m = 1.5$), the non-uniformity decreases as $\frac{R_c}{d}$ increases; on the other hand, for some other values of m (e.g. $m = 1$), the related non-uniformity increases as $\frac{R_c}{d}$ increases. This observation was never discovered in literatures and is quite different from what we observed from wafer.

3) The NU-surface is symmetric with respect to $m = 1$. When $\frac{R_c}{d} \approx 1$, as $|m| \to \infty$, the non-uniformity reaches a steady state $NU \approx 0.37$.

In general, as d increases (implies $\frac{R_c}{d}$ decreases) both the non-uniformity of wafer and polishing pad decrease. It supports the conclusion that increasing of d helps the improving the quality of polishing. Increasing the distance d also implies the increase of the size of polishing pad. However, polishing pad is one of the main cost in CMP. It may restrict the selection of d.

Note that Some other additional kinematic factors of CMP may also can to be considered to improve the non-uniformity in addition to m and $\frac{R_c}{d}$, see for example [7].

III. Ring type polishing pad

The above discussions are based on changing the rotational speeds and the distance between the centers of carrier and platen. In this section, we are going to discuss the effect of polishing pad with a ring shape. The main difference of this ring type pad with traditional one is the change of contact area. By changing the contact area of ring type polishing pad we "wish" that we would be able to improve the polishing result from kinematic perspective.
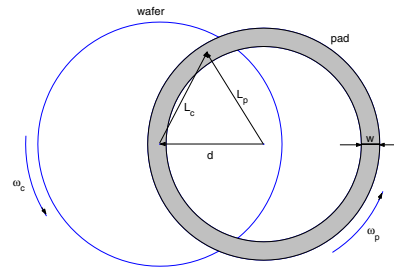

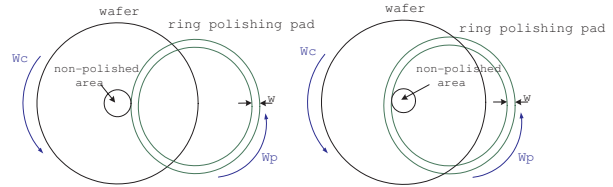Fig. 9. The schematic of ring type polishing pad

Fig. 10. There exists non-polished area on the wafer surface if $R_p + w < d$ or $d < R_p$

Figure 9 illustrates the structure and kinematic variables of the ring type polishing pad system, in which $\vec{L}_p$ and $\vec{L}_c$

are the position vector of contact point p on the ring relative to the center of polishing pad and wafer respectively, d is the distance between the centers of wafer and ring type polishing pad, w is the width of the ring, and $\vec{\omega}_p$ and $\vec{\omega}_c$ are the rotational velocity of pad and wafer respectively. Here we assume that

$$w \ll R_p. \tag{3.1}$$

where R_p is the inner radius of pad. Obviously, if the center of the wafer is not under the contact area of the ring type polishing pad, then there will exist a non-polished area on the wafer surface (See Fig. 10). Therefore, the distance between centers must be larger than the inner radius of ring and smaller than the outer radius,

$$R_p \leq d \leq R_p + w, \tag{3.2}$$

or,

$$1 \leq \frac{R_p}{d} \leq 1 + \frac{w}{d}. \tag{3.3}$$

If we assume that the rotational speed of pad is much higher than the carrier, that is,

$$|m| \gg 1, \tag{3.4}$$

then the magnitude of relative velocity of contact point p, V, can be approximated by the following

$$\begin{aligned} V &= \omega_c d \left\| (m-1)\rho_c \vec{e}_c + m\vec{i} \right\|, \\ &\approx \omega_c |m| d \left\| \rho_c \vec{e}_c + \vec{i} \right\|. \end{aligned} \tag{3.5}$$

Note that from Fig. 9 it is easy to obtain the following relationship

$$\rho_c \vec{e}_c + \vec{i} = \rho_p \vec{e}_p. \tag{3.6}$$

In addition, because of (3.1), we have $\rho_p \approx \frac{R_p}{d}$, it follows that the dimensionless relative velocity on contact area can be given by

$$\frac{V}{\omega_c d} \approx |m|\rho_p \approx |m|\frac{R_p}{d} \approx |m|, \tag{3.7}$$

where we have applied the assumptions (3.3) and (3.1). This implies the relative velocity at any point on the contact surfaces between ring and polishing pad will be approximately equal to a constant. This can be observed from Fig. 11, where we assume $m = 10$ and $\frac{w}{d} = 0.1$ respectively.

From Fig. 12, we can see that for a period of elapsed time T, the actual contact time at a particular contact point, $T_c(\rho_c)$, is

$$T_c(\rho_c) = T\frac{2\psi(\rho_c)}{2\pi}. \tag{3.8}$$

It can be proved that $\psi(\rho_c)$ can be determined by

$$\psi(\rho_c) = \begin{cases} \cos^{-1}\dfrac{\rho_c^2 + 1 - \left(\frac{R_p + w}{d}\right)^2}{2\rho_c} \\ \quad - \cos^{-1}\dfrac{\rho_c^2 + 1 - \left(\frac{R_p}{d}\right)^2}{2\rho_c}, \quad \text{for } \rho_c > \frac{w}{d}, \\ \pi, \qquad\qquad\qquad\qquad\qquad \text{otherwise,} \end{cases} \tag{3.9}$$
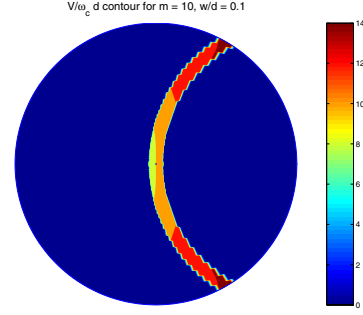

Fig. 11. The distribution of relative velocity at an instant on the wafer
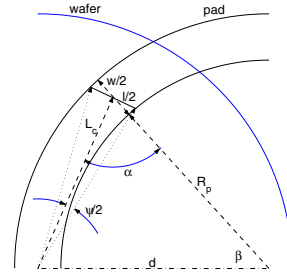

Fig. 12. The definitions of variables used for ring type polishing pad

Meanwhile if $\frac{w}{R_p} \ll 1$ equation (3.9) can be approximated by

$$\psi(\rho_c) = \begin{cases} 2\tan^{-1}\dfrac{l/2}{L_c} \approx 2\tan^{-1}\dfrac{\frac{w}{d}}{2\sin\beta}, & \text{for } \rho_c > \frac{w}{d}, \\ \pi, & \text{otherwise,} \end{cases}$$

in which l is the length of the segment perpendicular to $\vec{L}_c$ at contact point p and intersecting with pad, and β is the interior angle between $\vec{R}_p$ and $\vec{d}$,

$$\beta(\rho_c) = \cos^{-1}\frac{\rho_p^2 - \rho_c^2 + 1}{2\rho_p} \approx \cos^{-1}\frac{(\frac{R_p}{d})^2 - \rho_c^2 + 1}{2\frac{R_p}{d}}$$

Hence, for a period of elapsed time T, the dimensionless sliding distance is

$$\begin{aligned} S_n(\rho_c, \theta, m) &\triangleq \frac{1}{\omega_c dT}\int_0^{T_c(\rho_c)} V\,dt, \\ &= \frac{1}{T}\int_0^{T_c(\rho_c)} \|(m-1)\rho_c\vec{e}_c + m\vec{i}\|\,dt, \\ &= \frac{2|(m-1)\rho_c + m|}{\omega_c T} \\ &\quad \cdot \int_{\frac{1}{2}\theta}^{\frac{1}{2}[\omega_c T_c(\rho_c) + \theta]} \sqrt{1 - k_c \sin^2(\tau)}\,d\tau, \end{aligned} \tag{3.10}$$

where the parameter k_c is defined by (2.14). In the steady state,

$$\begin{aligned} S_{ns}(\rho_c, m) &\triangleq \lim_{T \to \infty} S_n(\rho_c, \theta, m) \\ &= |(m-1)\rho_c + m|\frac{\psi(\rho_c)}{\pi}a_0, \end{aligned} \tag{3.11}$$

where a_0 is given by (2.15). For the case $m \gg 1, \frac{w}{d} \ll 1$, we have

$$S_{ns}(\rho_c, m) \approx \begin{cases} \frac{2|m|}{\pi} \tan^{-1} \frac{w/d}{2 \sin \beta}, & \text{for } \rho_c > \frac{w}{d} \\ |m|, & \text{otherwise} \end{cases}. \quad (3.12)$$
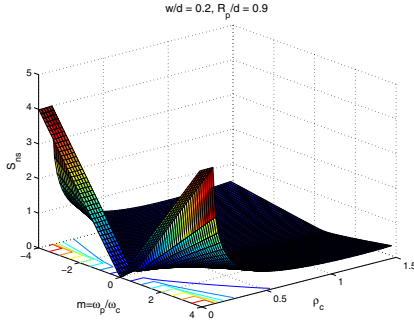

Fig. 13. $S_{ns}(\rho_c, m)$ on wafer when polished by a ring pad

Fig. 13 shows the normalized sliding distance distribution vs m and ρ_c. Fig. 14 depicts the difference between the exact and approximated expression for S_{ns}, as we can tell from this figure these two matches quite well. Note that S_{ns} on the wafer is not perfectly symmetric with respect to $m = 0$. Although the sliding distance, S_{ns}, in the outer region is much more robust to the variation of m than the wafer polished by traditional pad is, the material removed in central part of wafer will be much higher than that of the rest part. This result turns out not as good as we expected.
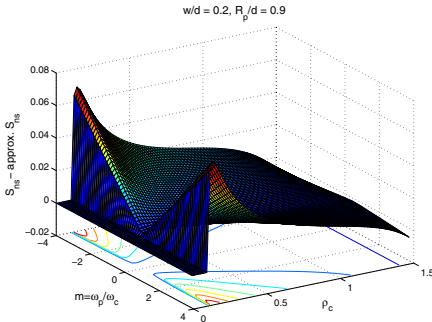

Fig. 14. S_{ns} using (3.11) - S_{ns} using (3.12)

Finally, use the previously defined non-uniformity (2.22), we have

$$\text{NU}(\frac{R_c}{d}, m) \triangleq \frac{\text{std}(S_{ns}(\rho, m))}{\text{mean}(S_{ns}(\rho, m))}, 0 \leq \rho \leq \frac{R_c}{d}, \quad (3.13)$$

As we have expeced from the distribution of sliding distance, the NU of wafer is very poor (see Fig. 15).

IV. CONCLUSION

In this paper, we analyze the non-uniformity of sliding distance on both wafer and polishing pad from kinematic point of view. It is shown that the steady state non-uniformity is determined by two parameters, m and $\frac{R_c}{d}$.
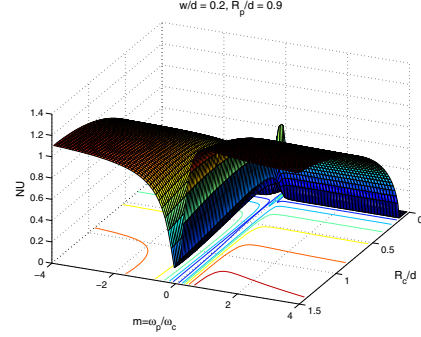

Fig. 15. NU of $S_{ns}(\rho_c, m)$ on wafer when polished by a ring pad

For a fixed ratio of $\frac{R_c}{d}$, the steady state non-uniformity distribution is an elliptic integral function of m. Roughly speaking, we find that the non-uniformity of wafer increases with $|m|$ and $\frac{R_c}{d}$. While negative m produces much larger non-uniformity than positive one. An important observation for polishing pad is that in two certain ranges of the ratio m, the larger $\frac{R_c}{d}$ produces on the contrary the smaller non-uniformity, this was never discovered in literatures to the knowledge of author. Then a ring type polishing pad was proposed for the intension of improving the non-uniformity of both wafer and pad. However, it turns out that the result is much worse than the traditional mechanism.

In the future, other mandatory factors including pressure distribution, interaction with slurry, etc. will be taken into account step by step.

REFERENCES

[1] H. Hocheng, H. Y. Tsai, and M. S. Tsai, "Effects of kinematic variables on nonuniformity in chemical mechanical planarization," *International Journal of Machine Tools & Manufacture*, vol. 40, pp. 1651–1669, 2000.

[2] S. R. Runnels, I. Kim, J. Schleuter, C. Karlsrud, and M. Desai, "A modeling tool for chemical-mechanical polishing desidn and evaluation," *IEEE Transactions on Semiconductor Manufactoring*, vol. 11, pp. 501–510, August 1998.

[3] H. Hocheng and H.-Y. Tsai, "A kinematic analysis of cmp based on velocity model," in *Conference on Chemical-Mechanical Polish(CMP) Planarization for ULSI Multilevel Interconnection (CMP-MIC)*, pp. 277–280, February 13-14 1997.

[4] F. W. Preston, "The theory and design of plate glass polishing machines," *Journal of the society of glass technology*, vol. 1, pp. 214–256, December 1927.

[5] J. feng Luo, D. A. Dornfeld, Z. Mao, and E. Hwang, "Integrated model for chemical-mechanical polishing based on a comprehensive material removal rate," in *Sixth International Conference on Chemical-Mechanical Polish (CMP) Planarization for ULSI Multilevel Interconnection (CMP-MIC)*, (Santa Clara, CA, U.S.A.), March 2001.

[6] Y. Moon, *Mechanical aspects of the material removal mechanism in chemical mechanical polishing*. PhD thesis, University of California at Berkeley, 1999.

[7] K. H. Wang, "The kinematic analysis of chemical mechanical polishing," Master's thesis, Dept of Aerospace Engineering, TamKang University, Tamshui, Taipei County, Taiwan, R. O. C., 2002.

[8] D.-Z. Chen and B.-S. Lee, "Pattern planarization model of chemical mechanical polishing," *Journal of The Electrochemical Society*, vol. 146, no. 2, pp. 744–748, 1999.

[9] J. Kim and H. Jeong, "Effects of process conditions on uniformity of velocity and wear distance of pad and wafer during chemical mechinal planarization," *Journal of Electronic Materials*, vol. 33, pp. 53–60, January 2004.